73rd International Astronautical Congress (IAC), Paris, France, 18-22 September 2022.

IAC-22-B1.IPB

ANALYSIS OF THE SPREAD OF THE CALLAO OIL SPILL OFF THE COAST OF LIMA, PERU USING EARTH OBSERVATION DATA

Zahra Okba[a]*, Eva Fernandez Rodriguez[b], Zachary Rowland[c], Lisah Ligono[d]

[a] *University Ibn Zohr, Agadir, Morocco,* zahra.okba@edu.uiz.ac.ma
[b] *Research department, AIOFAR,* eva.fernandez.aiofar@gmail.com
[c] *Remote sensing research department, AIOFAR,* zach.rowland.aiofar@gmail.com
[d] *Remote sensing research department, AIOFAR,* lisah.ligono.aiofar@gmail.com
* Corresponding Author: zahra.okba@edu.uiz.ac.ma

Abstract

The Humboldt Current System (HCS) is one of the most productive marine ecosystems in the world. In this current system, the upwelling of cold, nutrient-rich water drives the production of planktonic organisms which make up the base of the food web.

This paper analyses data associated with the Callao oil spill off the Peruvian coast, caused by tidal waves created by the 2022 eruption of the Hunga Tonga volcano in the South Pacific. The spillage of oil into the marine ecosystem has caused damage to natural resources and has had significant negative socio-economic consequences.

The areas of upwelling are directly influenced by regional wind patterns. Winds and waves are two key driving forces that cause upwelling phenomena in coastal areas and the open oceans. During oil spill events, oil slicks cover the ocean surface and thus change the surface roughness and affect the Ekman transport by minimizing the wind effect on the ocean surface. These effects are characterized in this research.

The methodology considered in this study is to analyze the impact and evolution of the oil spill on a sample of three different sites off the coast of Lima, Peru. Synthetic Aperture Radar (SAR) imagery is analyzed to identify and track the exact location of the spills. To assess the environmental impact, the following parameters are used and analyzed in the areas of study to assess their influence on other variables: sea surface temperature (SST), chlorophyll (CHL), nitrates (NO3) levels, upwelling index (Ekman transport based), and wind speed.. The correlations between these parameters are characterized to provide a better understanding of their relative influences and the potential consequences of oil spills.

The results enable the forecasting of the oil spill trajectory and movement off the coast of Peru, and the prediction of its environmental impacts on marine life and socio-economic impact on aquaculture activities. This study allows for refined modeling of oil spills, enabling a better understanding of spill evolution using environmental and remote sensing data.

Keywords: oil spill, Callao, Humboldt Current System, Upwelling, Ekman transport

Acronyms/Abbreviations

HCS Humboldt Current System
SAR Synthetic Aperture Radar
SST Sea Surface Temperature
CHL Chlorophyll
NO3 Nitrates
BAT Bathymetry

1. Introduction

Almost 12000 barrels of crude oil were spilled into the Pacific Ocean off the coast of Lima, Peru, on the 15th of January 2022. The spill occurred at La Pampilla refinery which belongs to the energy company Repsol and is located north of Callao (Fig. 2), some 30 kilometers from the country's capital. The big waves of the tsunami that originated from the eruption of the undersea Hunga-Tonga Hunga-Ha'apai volcano in Tonga might have caused damage to a tanker unloading oil at the refinery and precipitated the disaster.

The oil was estimated to spread more than 106 square kilometers and caused the death of 491 specimens of wildlife according to the Peruvian National Forestry and Wildlife Service [1]. The Humboldt current, also called the Peru Current (Fig 1), carried the oil north affecting nearby waters and shorelines. The Peruvian upwelling system is located along the western coast of South America, approximately between 20°S and 5°S and 90°W and 70°W, and causes strong coastal upwelling with equatorial winds. Together with the Benguela, Canary, and California systems, the Peruvian upwelling system is one of the four most important coastal upwelling regions in the world. These four upwelling systems are highly productive. The Humboldt current connects the cold waters of the Southern Ocean to the warm currents of the equatorial Pacific [2] leading to one of the most productive marine ecosystems in the world. The production volume fluctuates greatly and is highly dependent on environmental factors such as sea surface

temperature and ocean currents. In this region, El Niño contributes significantly to environmental change [3].

Due to the importance of the environment linked to the Humboldt current system, the oil spill originating at La Pampilla has an enormous ecological impact.

In addition, the artisanal fishing local economy is also highly affected by the spill after having lost their main source of income. Some other businesses which depend on the fishing industry are also impacted such as restaurants, food vendors, or those who rent boats.

This paper aims to analyze the evolution of oceanographic and atmospheric parameters in the first 4 months of this oil spill event in order to explain the chronology of the reported oil hits on the Callao coast. In addition, by investigating wind and wave movement near the coast, we intend to discuss the effect oil has on upwelling activity and chlorophyll.

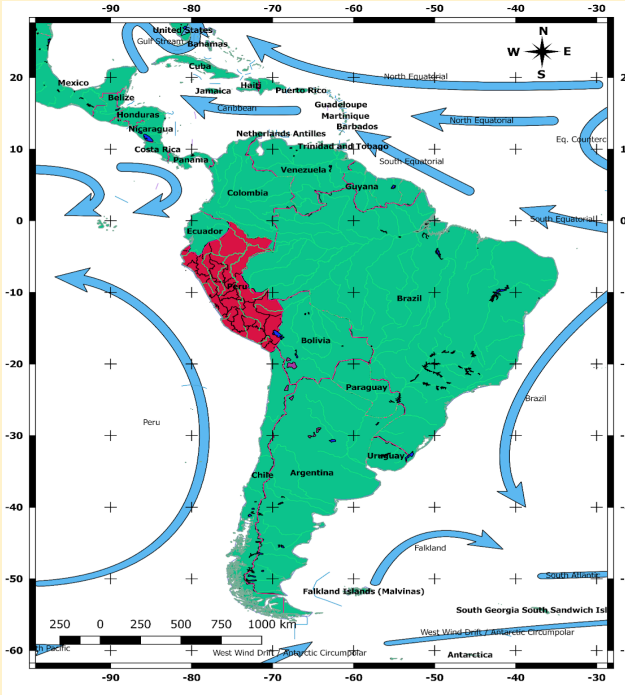

Fig. 1. The geographic location of Peru and Peruvian current

2. Material and methods

2.1 Area of Study

Callao Bay is located on the central coast of Peru, within the Lima metropolitan area, and belongs to the Constitutional province of Callao (Fig 2). It serves as one of the most important Peruvian bays due to the economic activities related to Peru's biggest port, the Terminal Port of Callao (TP-Callao), located to the south of the Rimac River estuary.

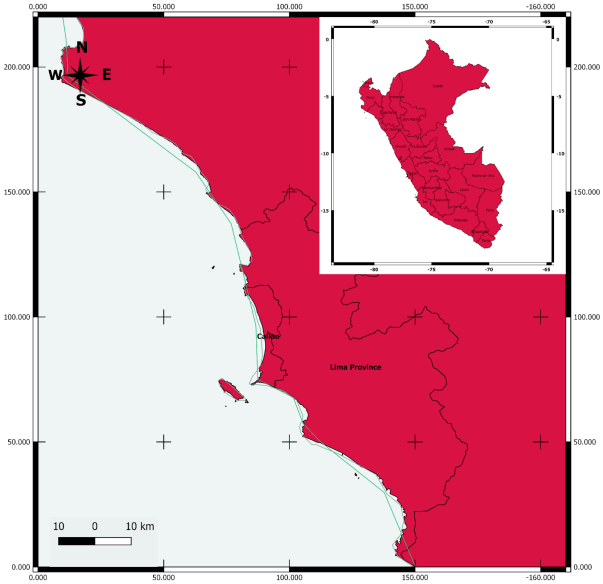

Fig. 2 The geographic location of the Peruvian oil spill

2.2 Data sets

2.2.1 Upwelling index data

ERD (oceanographic data server at NOAA) has been updating the Bakun upwelling Index every 6 hours at the designated location from 2021 to 2022. To calculate the upwelling index in this study we use the package xtractomatic [4], package on R. We define a function 'upwell' that rotates the Ekman transport value to get the offshore component (upwelling index), and also defines a function plotUpwell that plots the upwelling. xtracto_3D can download Ekman transport calculated from the pressure field of the Fleet Numerical Meteorological and Oceanographic Center (FNMOC). Upwelling Index (UI) can be defined as the Ekman transport component in the direction perpendicular to the coastline [5] following:

$$UI = -(\sin(\theta - \pi/2)\, Q\, x + \cos(\theta - \pi/a2)\, Q\, y)$$

where u is the angle between the coastline and the equator (on average, $\theta = 74$ is considered in the Peruvian region). Positive (negative) upwelling indices correspond to upwelling-favorable (unfavorable) conditions. Six hourly wind data were converted to UI and then averaged monthly.

2.2.2 Wind satellite data

The forcing field for the upwelling dynamics is wind stress [6]. The data used in this study for the wind speed and direction has been extracted from the "ERA5 hourly data on single levels from 1959 to present" dataset available through the Copernicus Climate Change Service (C3S) Climate Data Store (CDS) [7]. A specific

location point has been identified as a representation of the wind condition with a latitude of -11.66º and a longitude of -77.39º. The reason for this selection is the availability of data in the selected dataset for this point, the closeness to the source of oil, and its position in front of the ocean shoreline.

In the area of interest, wind generally blows equatorward along the eastern ocean boundary, so the Ekman transport drives surface waters away from the Peruvian coast. To study the condition during the oil spill disaster both wind speed and direction have been analyzed.

The parameter selected to study the wind speed is the 10-meter wind speed which is defined as the horizontal speed of the "neutral wind" at a height of 10 meters above the surface of the Earth. The wind direction is analyzed through the 10-meter wind direction defined as the direction from which the "neutral wind" blows at a height of 10 meters above the surface of the Earth. The neutral wind is in the direction of the surface stress and it is calculated from the surface stress and roughness length by assuming that the air is neutrally stratified.

2.2.3 Ocean waves data

The data used in this study for the wave period and direction has been extracted from the "ERA5 hourly data on single levels from 1959 to present" dataset available through the Copernicus Climate Change Service (C3S) Climate Data Store (CDS) [7]. As for the case of wind speed and direction, a specific location point has been identified as a representation of the wind condition. This location is the same as for the wind case.

The parameter selected to study the ocean wave direction is the mean wave direction parameter defined as the mean direction of ocean/sea surface waves. The ocean wave period is analyzed through the mean wave period parameter defined as the average time it takes for two consecutive wave crests, on the surface of the ocean/sea, to pass through a fixed point. For both parameters, the mean over all frequencies and directions of the two-dimensional wave spectrum is studied considering a combination of waves with different heights, lengths, and directions. Furthermore, the parameters take account of both the wind-sea and swell waves.

3. Results and discussion

3.1 Oil spill tracing

As in Fig. 5, the oil spill spread several days after the collision in a southward direction from the source of the oil spill. The movement goes to the south along the coast from February to March. This can be caused by the wave and wind movement and direction.

As can be seen from Fig. 3, the wave front mainly travels south along the Peruvian coast (~205º) with slight turns to the west in the first days of February. . Fig. 4 shows a declining trend of the wave period between January and April, varying from 8.5s in January to 8s in March, with the longest wave period registered in February varying from 10s and 12.4s.

Therefore, the waves could be held responsible for transporting the oil to the south towards the beach along the coast.

La Pampilla oil spill took place in January, during a season usually exposed to decreasing wind action and upwelling activity. Thus, it is possible that oil will be sedimented and accumulated, then potentially covered by sediments over time and re-exposed with the erosion of the seabed.

According to [8], bathymetric characteristics are able to alter ocean circulation and oil spill trajectories in offshore oil spills. Fig. 6 shows the bathymetric patterns in the Peruvian coast of interest using the Gridded Bathymetry Data provided by the General Bathymetric Chart of the Oceans (GEBCO).

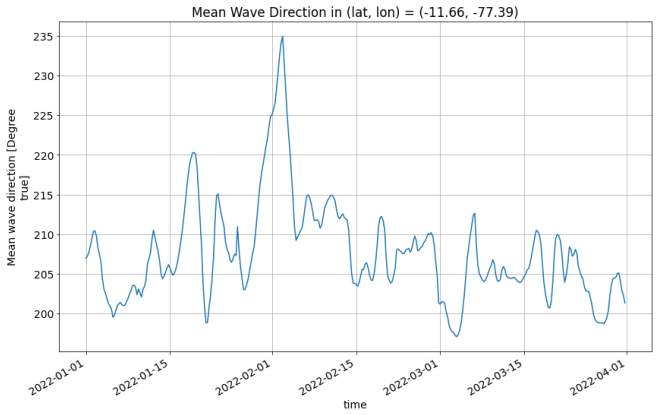

Fig. 3. Mean wave direction on the Peruvian coast

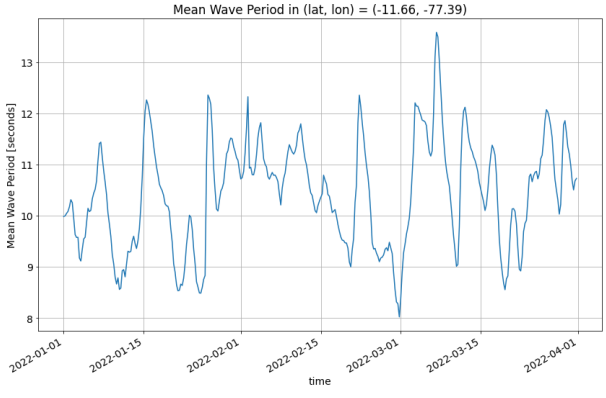

Fig. 4. Mean wave period on the Peruvian coast

Oil spill movements were tracked using the 'SAR oil-spill mapping using the pseudo-anomaly approach' from the World Bank Group. Oil spills can be spatially

detected and mapped using SAR data as, in high wind speed conditions, the oil surface damping decreases as the vitality of ocean waves increases, with oil beginning to get blended with waves. As soon as the oil is spilled, it begins to spread against the ocean surface. This property is illustrated in Fig. 5. where the darker areas of the water surface show greater surface reflectivity to radar, indicating the presence of oil on the surface.

SAR data for this study was obtained from Sentinel-1A only, due to the interruption in data from Sentinel-1B caused by the anomaly and subsequent decommissioning of the satellite, as well as the high spatial resolution (10 m) of the Sentinel-1 data in general. VV polarization in the ascending pass direction was used due to the availability of data.

A small region southwest of the spill was used as a reference for normal conditions (using mean pixel values in the year before the spill event, from 2021-01-01 - 2022-01-01) to calculate the red oil spill masks in Fig. 5. The result is the four images in Fig. 5. that track the spatial movement of the spill during the event, on dates where data is available from the satellite.

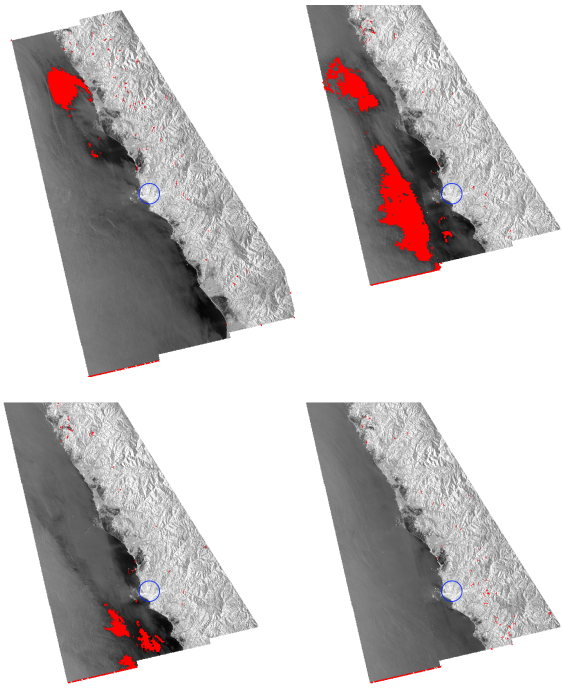

Fig. 5. Sentinel-1A SAR images with oil spill surface estimation masked in red and Lima highlighted with a blue circle (imagery from the following dates: top left 02/02/2022, top right 26/02/2022, bottom left 10/03/2022, bottom right 22/03/2022)

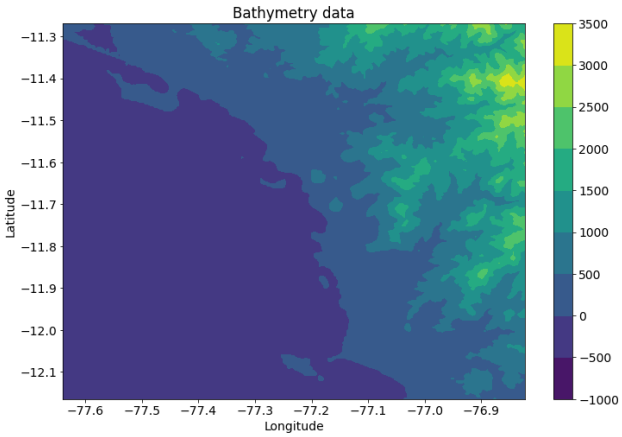

Fig. 6. Bathymetric patterns on the Peruvian coast

3.2 Upwelling response to oil spill

Several factors affect the diffusion of spilled oil such as tidal flow, weather conditions, wave movement, and biochemical reactions. The most significant of those to determine the oil spill movement are tidal currents, wind, and waves [9]. The effect of wind, tidal currents, and wave movement was investigated in [9] for the Hebei Spirit oil spill in the Yellow Sea in 2007 using simulated data. Their results refute that wind and waves were the most relevant factors for oil spill diffusion leading to the coast.

Therefore, this paper explores the observations for these parameters as well as some additional data to assess the oil spill development. Specifically, the impact of the oil spill is measured through water quality parameters for which both the seasonal trend and the changes before and during the oil spill are analyzed to distinguish the precise changes driven by the spill.

The authors in [10] found that the wind-driven Ekman current was overestimated by 75 to 100% due to the changes in the effective wind speed during the observations from the Deepwater Horizon oil spill in 2010. This bias can affect the trajectory prediction and, consequently, the effectiveness of the mitigation strategies planning.

The Peruvian upwelling system (PUS) is the most productive marine ecosystem among the Eastern Boundary upwelling Systems. The trade wind system of the South Pacific drives a nearly continuous upwelling which is subjected to variations on a wide range of times scales. The intensity and variability of upwelling control crucially the nutrient supply to the euphotic surface layer and thus, the overall productivity of the system.

As can be seen from Fig. 7, the Ekman-based upwelling index is favorable (positive value) but less intense than the usual values identified for the area through the literature review. This indicates that the irregularity of wind direction and intensification of wind

speed is not strong enough to keep the Ekman transport active for a longer period.

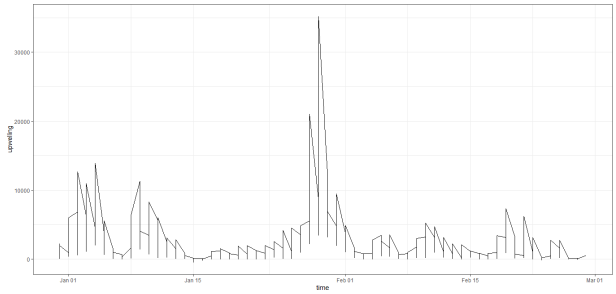

Fig. 7 the upwelling index UI, calculated from Ekman transport of the Peruvian coast

The Sea Surface Temperature (SST) parameter evolution permits the assessment of thermic changes that the spill brings. Fig. 8 shows the seasonal trend of this parameter where the maximum temperatures occur during the first months of the year, typically in February.

Based on Fig. 8 the SST gets lower between June and October reaching 15.5ºC, and higher between November and May reaching 22.4ºC. Between 2019 and 2022, the SST declined by 1.2ºC during the period it gets lower and increased by 1ºC during the period it gets higher.

A more detailed study of the SST during the spill for latitude -11.66º and longitude -77.39º returns the results in Fig. 9. The latter is relevant to highlight an abrupt decrease in temperature, 1.3ºC approximately, around the 22nd of January. Even though the SST reached 20.75ºC during the disaster, the ocean water still followed its seasonal trend and got colder in February and even colder until April, which can be referred to as upwelled cold water that originated through upwelling activity.

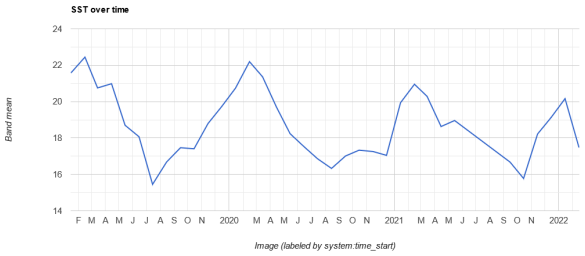

Fig. 8. Sea Surface Temperature parameter evolution in degrees (ºC) for 2019, 2020, 2021, and part of 2022 on the Peruvian coast. This data has been extracted from MODIS-Aqua measurements.

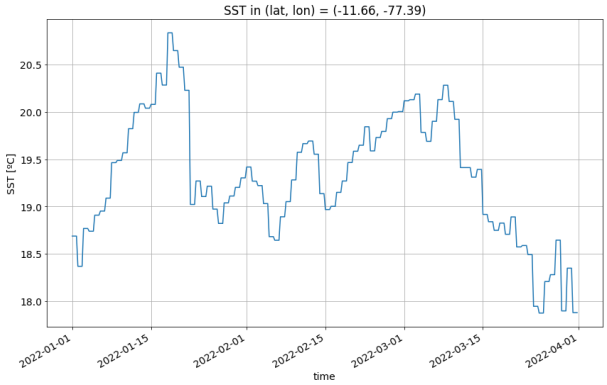

Fig. 9. Sea Surface Temperature parameter evolution in degrees (ºC) for January, February, and March 2022 for latitude=-11.66º and lon=-77.39º. The data has been extracted from the "ERA5 hourly data on single levels from 1959 to present" dataset in the Copernicus Climate Change Service (C3S) Climate Data Store (CDS)

According to [11], the surface water moves at 2-5% of the wind speed and, theoretically, is deflected to the right (left) of the wind direction in the Northern (Southern) hemisphere by Coriolis and frictional forces.

In Fig. 10 the 10-meter wind speed from the "ERA5 hourly data on single levels" is shown as a representative point in the area under study during the oil spill on the Peruvian coast. This parameter refers to the horizontal speed of the "neutral wind" at a height of 10 meters above the surface of the Earth. From the graph, it can be seen that wind speed is moving in a range between 2 and 5.5 m/s approximately which can be an obstacle for the upwelling to be more intense, the minimum wind speed required is 5m/s. The low wind speed explains the intensity of the upwelling index observed in Fig. 10 in January.

Apart from the speed, another important aspect related to the wind to determine the oil spill movement is its direction. Fig. 11 shows the 10-meter wind direction parameter from the "ERA5 hourly data on single levels" for a representative point in the area under study during the oil spill on the Peruvian coast. This parameter refers to the direction from which the "neutral wind" blows, in degrees clockwise from true north, at a height of 10 meters above the surface of the Earth.

The wind direction is an essential feature of the upwelling phenomenon. Specifically, the wind must be parallel to the coast for the upwelling to occur. From Fig. 11, it is clear that the wind direction in the months of the Peruvian coast oil spill was mainly blowing to the south (180º) with slight turns to south-west and south-east which is not parallel to the coast.

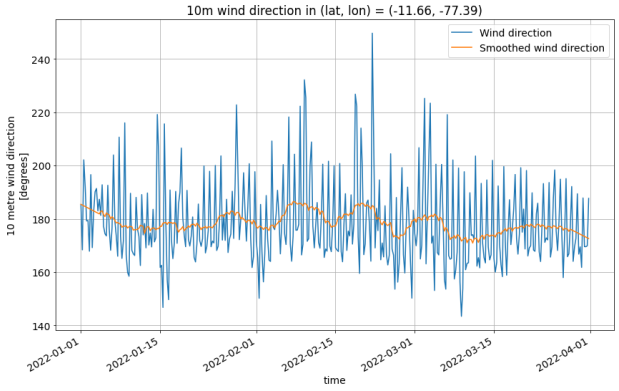

Fig. 10. 10-meter wind speed parameter evolution in m/s for January, February, and March 2022 for latitude=-11.66º and lon=-77.39º.

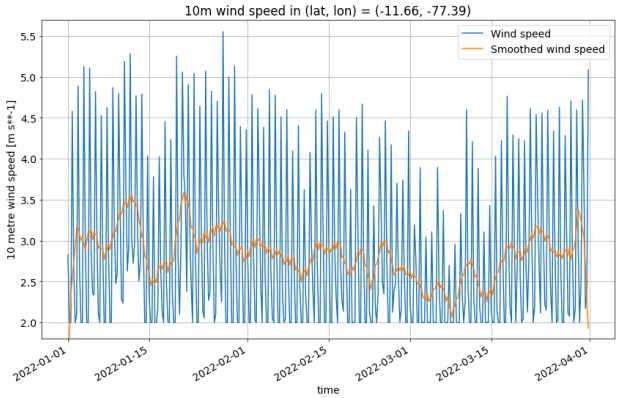

Fig. 11. 10-meter wind direction parameter evolution in degrees for January, February, and March 2022 for latitude=-11.66º and lon=-77.39º.

3.3 Nutrient response

During the upwelling event, the upwelled water brings with it essential minerals for the ecosystem and more precisely for phytoplankton growth, and nitrate is one of the most important substances that are crucial for phytoplankton growth. According to Fig. 9, the SST was observed at its lowest after the 15th of March which coordinates with the concentration of nitrate shown in Fig. 12, with a high concentration of 12 mmol/l and lowest concentration of 5.6 mmol/1 while the oil spill event.

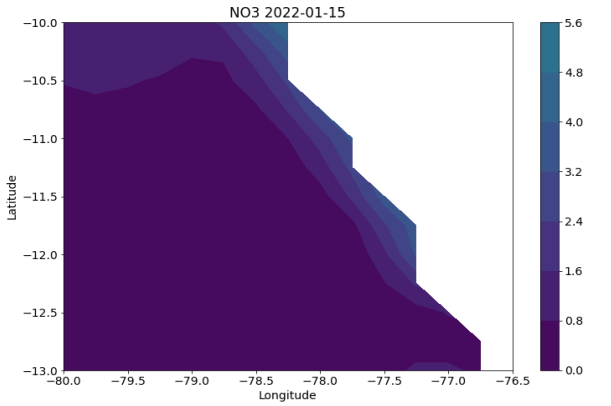

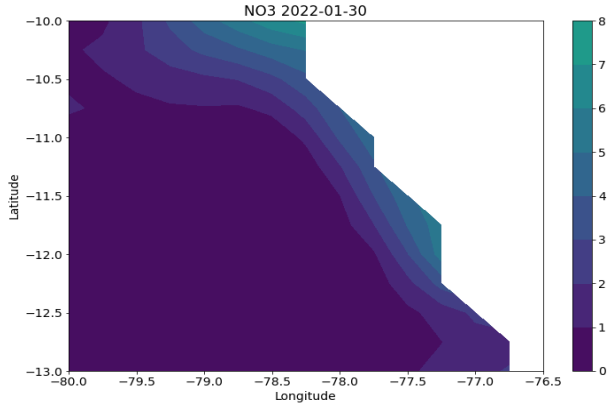

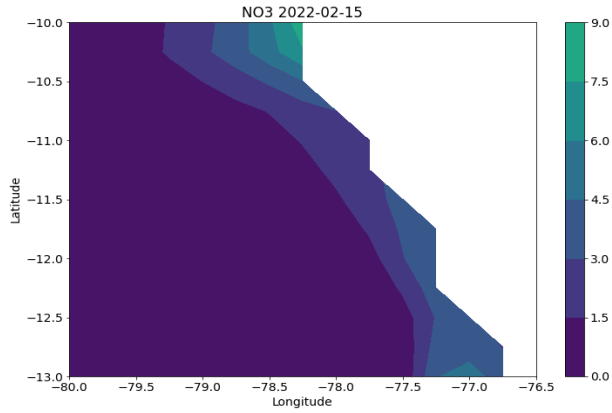

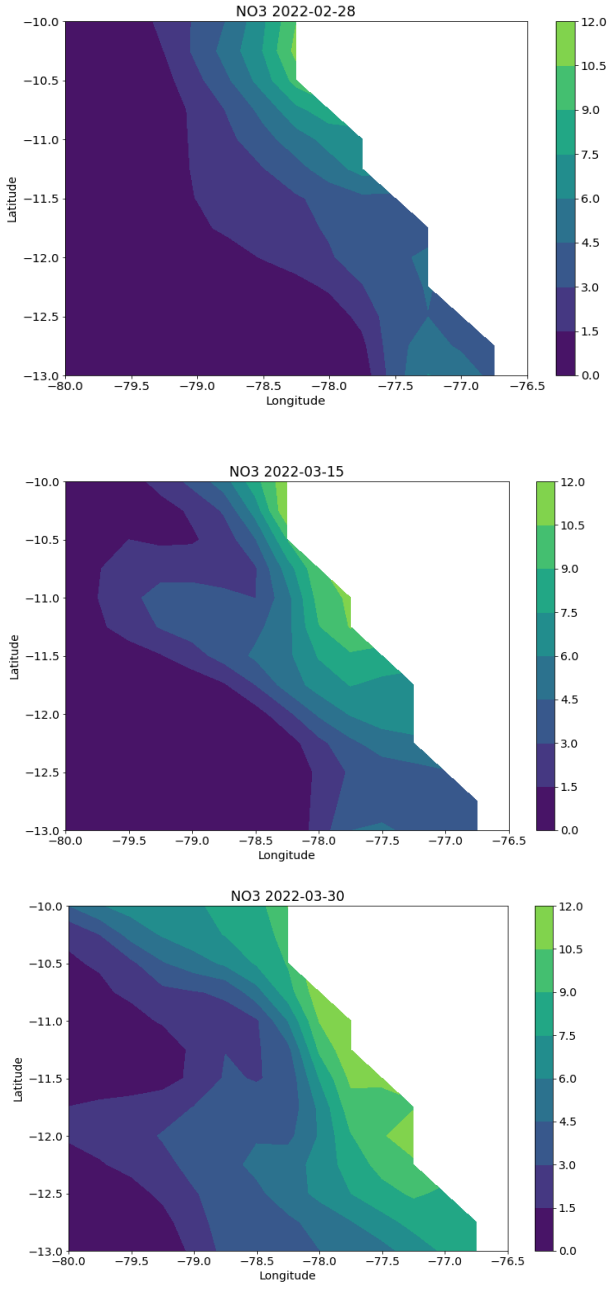

Fig 12. The NO3 concentration imageries for January, February, and March in 2022.

Several studies have found phytoplankton biomass increases only after the relaxation of upwelling activity [12]. It seems that a relaxation period is required for bloom initiation, to allow underwater light levels and depleted phytoplankton cells to increase [12].

The results indicate weak favorable upwelling signals in temperature profiles (see Fig. 9) and high subsurface maxima in the Chla survey before the oil spill event and one month after it with a value of 4.8mg/m3 (see Fig. 13). The highest Chl-a values (4.8 mg m3) were concentrated between -10N and -10.5N and between -11.3N and 12.3N, but intermediate values (2.4 mg m3 – 1.8 mg m3) extended offshore during the first of January. As shown in Fig. 13, the lowest Chl-a values (1.2 mg m3) were concentrated during the oil spill event along the coast. Chlorophyll concentrations are enhanced inshore of the upwelling front (~ 5 mg m−3) compared to offshore (~ 0.6 mg m−3) due to nutrient-rich subsurface waters (12 mmol/1 NO3) that are brought to the surface in the coastal upwelling. As the minerals are upwelled with cold water essential for phytoplankton growth also the relaxation of the water is important for proliferation. The high concentration of Chl-a on the 15th of February is explained by the upwelling event on the 1st of February and its relaxation which gave the phytoplankton the condition for its growth.

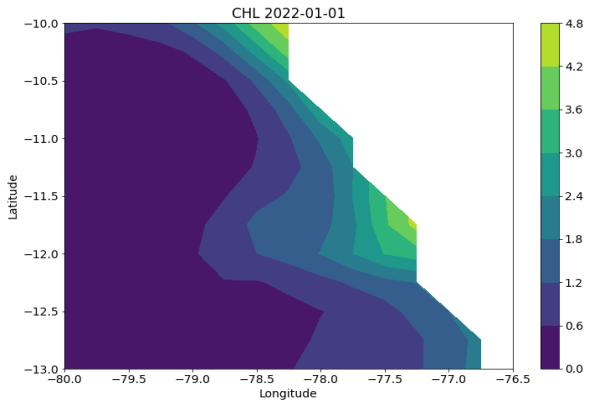

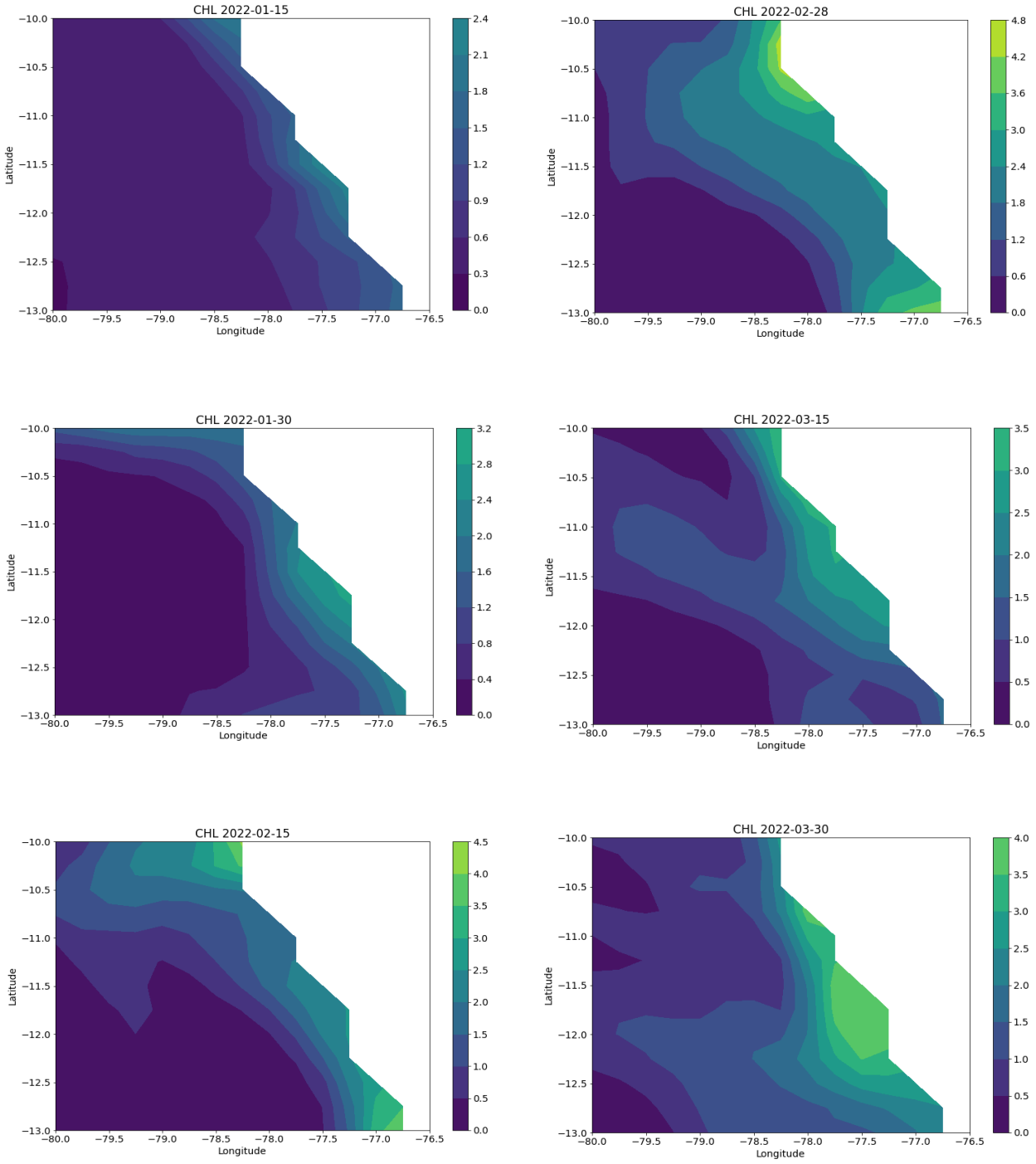

Fig 13. The Chl-a concentration imageries for January, February, and March in 2022.

4. Conclusions

After the analysis included in this study, future lines of research will cover the oil spill movement gaps of the satellite radar image using the wind speed and direction data. These gaps in the satellite imagery are explained through the relatively high revisit time of the Earth Observation satellites. The introduction of alternative methods for movement prediction allows for better monitoring of the oil spill.

The movement of the oil spill along the Peruvian coast towards the south is explained in the paper by wind and wave activity.

The upwelling event activity was at a low intensity which is caused by the unregulated wind speed and direction. Also, the thickness of the oil on the surface of the water can explain the low activity of the upwelling.The upwelled nitrate with cold water was in a low concentration during the oil spill event and the values increased after that, and it was synchronized with the concentration of chlorophyll along the coast.This study has demonstrated the applicability of readily available environmental and remote sensing data for the rapid mapping of oil spill disasters.

References

[1] weworld, “Peru oil spill: an unprecedented ecocide in the country,” *5 april 2022*. https://www.weworld.it/en/news-and-stories/news/peru-oil-spill-an-unprecedented-ecocide-in-the-country.

[2] Territorial Agency, “Humboldt Current.” https://ocean-archive.org/collection/156.

[3] P. Penven, J. Pasapera, J. Tam, C. Roy, D. Recherche, and U. D. B. Occidentale, “GLOBEC INTERNATIONAL NEWSLETTER OCTOBER 2003 GLOBEC SCIENCE A column for scientific notes of relevance to the GLOBEC community Modeling the Peru Upwelling System seasonal dynamics,” vol. 1, no. October, pp. 23–26, 2003.

[4] R. Mendelssohn, “xtractomatic: accessing environmental data from ERD’s ERDDAP server. R package version,” 2018. https://github.com/rmendels/xtractomatic.

[5] L. Nykjaer and L. Van Camp, “Seasonal and interannual variability of coastal upwelling along northwest Africa and Portugal from 1981 to 1991,” *J. Geophys. Res.*, vol. 99, no. C7, pp. 197–207, 1994, doi: 10.1029/94jc00814.

[6] J. Cushman-roisin, Benoit Beckers, “Book, Geophysical Fluid Dynamics Introduction to Physical and Numerical Aspects,” 2009.

[7] J.-N. Hersbach, H., Bell, B., Berrisford, P., Biavati, G., Horányi, A., Muñoz Sabater, J., Nicolas, J., Peubey, C., Radu, R., Rozum, I., Schepers, D., Simmons, A., Soci, C., Dee, D., Thépaut, “ERA5 hourly data on single levels from 1959 to present,” 2018. https://cds.climate.copernicus.eu/cdsapp#!/dataset/reanalysis-era5-single-levels?tab=overview.

[8] T. M. Alves, E. Kokinou, G. Zodiatis, R. Lardner, C. Panagiotakis, and H. Radhakrishnan, “Modelling of oil spills in confined maritime basins: The case for early response in the Eastern Mediterranean Sea,” *Environ. Pollut.*, vol. 206, pp. 390–399, 2015, doi: 10.1016/j.envpol.2015.07.042.

[9] K. H. Lee, T. G. Kim, and Y. H. Cho, “Influence of tidal current, wind, and wave in hebei spirit oil spill modeling,” *J. Mar. Sci. Eng.*, vol. 8, no. 2, pp. 1–18, 2020, doi: 10.3390/jmse8020069.

[10] H. Shen, W. Perrie, and Y. Wu, “Wind drag in oil spilled ocean surface and its impact on wind-driven circulation,” *Anthr. Coasts*, vol. 2, no. 1, pp. 244–260, 2019, doi: 10.1139/anc-2018-0019.

[11] N. M. Ridgway, “Direction of drift of surface oil with wind and tide,” *New Zeal. J. Mar. Freshw. Res.*, vol. 6, no. 1–2, pp. 178–184, 1972, doi: 10.1080/00288330.1977.9515415.

[12] P. C. Longdill, T. R. Healy, and K. P. Black, “Transient wind-driven coastal upwelling on a shelf with varying width and orientation,” *New Zeal. J. Mar. Freshw. Res.*, vol. 42, no. 2, pp. 181–196, 2008, doi: 10.1080/00288330809509947.